Layer Morphology Control in Ni/Ti Multilayer Mirrors by Ion-assisted Interface Engineering and B_4C Doping

Fredrik Eriksson,[1,*] Naureen Ghafoor,[1] Sjoerd Broekhuijsen,[1] Daniel Ostach,[2] Grzegorz Greczynski,[1] Norbert Schell,[2] and Jens Birch[1]

[1] Thin Film Physics Division, Department of Physics, Chemistry and Biology (IFM), Linköping University, SE-581 83 Linköping, Sweden
[2] Helmholtz-Zentrum Geesthacht, Centre for Materials and Coastal Research, Institute for Materials Research, Max-Planck-Straße 1, 21502 Geesthacht, Germany

Abstract

Ni/Ti is the materials system of choice for broadband neutron multilayer supermirrors. The reflected absolute intensity as well as neutron energy range from state-of-the-art mirrors are hampered by a Ni/Ti interface width, typically 0.7 nm (caused by nanocrystallites, interdiffusion, and/or intermixing), limiting the optical contrast across the interface as well as limiting the minimum usable layer thickness in the mirror stack.

In this work we explore elimination of nanocrystallites by amorphization through boron-carbon doping in combination with interface smoothening by modulation of ion-assistance during magnetron sputter deposition of individual Ni and Ti layers, ranging from 0.8 nm to 6.4 nm in thickness.

In situ high-energy synchrotron wide angle X-ray scattering (WAXS) revealed an effective hindering of Ni/Ti crystallization through a minute concurrent B_4C flux during growth. Post-growth X-ray reflectivity (XRR) confirmed the incorporation of B_4C but also showed that interface widths deteriorated when a constant substrate bias of -30 V was used. However, XRR showed that interface widths in B_4C-doped multilayers improved significantly, compared to those in pure Ni/Ti multilayers, by employing a two-stage substrate bias, where the initial 1 nm of each layer was grown with -30 V substrate bias, followed by -100 V bias for the remaining part of the layer.

The present results shows that B_4C doping of Ni/Ti multilayers leads to significantly smaller interface widths when combined with engineered interfaces through temporal control of the substrate bias. Consequently, a significant improvement of neutron supermirror performance can be expected by emplying this technique using ^{11}B isotope-enriched B_4C source material.

1. Introduction

Neutron scattering is a powerful tool for the study of condensed matter because the wavelengths and energies of thermal and cold neutrons (λ = 1 - 10 Å) match well to the length and energy scales of solids and liquids [ref]. Thus, there is a lot of information and many interesting phenomena to study using neutron scattering. The applicability of neutron scattering techniques, however, is limited by the relatively low flux of useful neutrons generated by today's research reactors or pulsed spallation sources, which is many orders of magnitude lower than the flux of X-rays produced by contemporary photon sources [ref].

Multilayer mirrors have proved to be key elements for …

The largest increase in neutron flux to the experiment is expected to come from improving the performance of different neutron optical components [1].

Ni/Ti neutron multilayer mirrors

Ni/Ti is the materials system of choice for broadband neutron multilayer supermirrors. The reflected absolute intensity as well as neutron energy range from state-of-the-art mirrors are

*Corresponding author: freer@ifm.liu.se
mobile: +46-707 315 139

hampered by a Ni/Ti interface width, typically 0.7 nm (caused by nanocrystallites, interdiffusion, and/or intermixing), limiting the optical contrast across the interface as well as limiting the minimum usable layer thickness in the mirror stack [2].

Neutron reflectivity theory – few sentences – SLD → Ni/Ti very attractive for neutron multilayer mirrors.
Neutron scattering length densities – large difference in real part, both small imaginary parts → high reflectivity by increasing the number of contributing layers/interfaces.

Layer morphology – roughness and intermixing/interdiffusion limits the performance. State-of-the-art = 7 Å, however improvement on an Å-level yields a significant reflectivity gain.

Even though the state-of-the-art interface width is as low as 7 Å [ref] the interfaces are still in need of special attention. Considering that the reflectivity is exponentially sensitive to the ratio of the interface width to the multilayer period squared, according to the Debye-Waller modification factor [ref], it is clear that even a slight improvement in interface width will have a significant gain in reflectivity. Furthermore, in order to realize higher m-value supermirrors, which require thinner layers to be deposited, the requirements on the interface width becomes increasingly demanding. Considering a neutron waveguide application, where the neutrons are reflected n times and the waveguide transmission depends on each reflection as $T = R^n$, the motivation for research on improving the interface definition becomes even stronger [ref]. As a numerical example, decreasing the interface width from 7 Å to 6 Å for a 100 m supermirror waveguide with an average of 14 reflections [ref], designed for m=8 and using a $z^{-1/4}$ layer thickness distribution [ref] with a minimum layer thickness of d Å, would increase each reflection from X % to Y %, corresponding to an increase in waveguide transmission by as much as Z %.

Supermirror structure? Depth-graded 40 nm→2 nm.

This study explores the possibility to introduce B_4C into the Ni/Ti multilayer structure and a temporal control of the substrate bias voltage during growth to change the layer morphology and interface definition to improve the neutron reflectivity performance.

[]

Theoretical considerations
Expected effects of B4C doping and substrate bias:
B forms very strong bonds with metals

Predicted enthalpy of formation and enthalpy of mixing of binary Ti and Ni compounds

	Ti ΔH^{for}_{calc} kJ/mol	Ti ΔH^{mix}_{calc} kJ/mol	Ni ΔH^{for}_{calc} kJ/mol	Ni ΔH^{mix}_{calc} kJ/mol
B	-84	-43	-33	-9
C	-77	-19	+21	+51
N	-146	-35	+36	+86
O	-	-	-244	-
Ni	-52	-35	-	-
Ti	-	-	-52	-35

Strong B-metal bonds limits interdiffusion [3], promotes amorphization [4], however it lowers the necessary adatom mobility required to produced smooth surfaces.
Substrate bias attracts ions from the plasma. Ions <~30 eVsurface displacements. Ions >~100 eV causes subsurface implantation.
Make some simple SRIM calculations of this (– to support the chosen values)!
The attracted ions stimulate the adatom mobility without causing any intermixing (using a modulated bias), and provides more dense layers with smooth surfaces.

2. Experimental details

Multilayer thin films of pure Ni/Ti and those doped with B_4C have been deposited onto Si (100) substrates using ion-assisted DC magnetron sputter deposition. The 600-mm-diameter cylindrical deposition chamber is equipped with four 75-mm-diameter sputter sources tilted with an angle of X° towards the substrate normal with a target-to-substrate distance of 150 mm. Between adjacent sputter sources high magnetic permeability μ-metal shielding is used to minimize cross contamination as well as to extend the magnetic field closer to the substrate. In front of the sputter sources fast-acting shutters allow for control of the sputtered flux and enables single layers, multilayers, as well as co-sputtered layers to be deposited.

The 10×10×0.5 mm^3 substrates were rotating around the sample normal at constant rate of 7 rpm, directly in line of sight of all sputter sources. The substrate table was electrically isolated enabling a negative substrate bias voltage to be applied during growth. Although substrate heating was available depositions were performed at ambient growth temperatures (< 50 °C). The chamber was evacuated to a base pressure of X Pa (Y Torr) using a dual turbo setup and was equipped with a loadlock to maintain a good vacuum and allow for easy sample exchange. The deposition system is described in more detail elsewhere [5].

Ultra-high purity argon gas (> 99.999998%) was introduced to a working pressure of 3 mTorr (0.4 Pa), as measured with a capacitance manometer. Target discharges were established with constant-power power supplies, and discharge powers of 20 W and 60 W, as measured with closed shutters, were used for Ni and Ti, respectively. This yielded Ni and Ti deposition rates of about 0.36 and 0.39 nm/s as determined from hard X-ray reflectivity measurements of single layer films. For B_4C discharge powers of 0, 17, 35, and 70 W were used.

Both single multilayer structures, with a period of 10 nm and 5 repetitions, and stacked multilayer structures, with periods of 1.6, 3.2, 6.4, and 9.6 nm consisting of correspondingly 32, 16, 8 and 6 repetitions, in order to maintain roughly the same total thickness of each multilayer stack, were deposited. The nominal Ni and Ti layer thicknesses were kept equal. The single multilayer structures have been deposited with two different designs of ion assistance and with different amounts of B_4C-doping, while for the stacked multilayer structures only the B_4C-doping was varied. The layer thicknesses were not adjusted for the amount of incorporated B_4C at different B_4C target powers and thus the multilayer period increase the more B_4C that is included. The composition of the films were evaluated using Elastic Recoil Detection Analysis.

Either a constant substrate bias voltage of -30 V was applied, or a two-stage modulated substrate bias was employed, where the initial 1 nm of each layer was grown with -30 V substrate bias, followed by -100 V bias for the remaining part of the layer. The latter ion assistance design has proven successful in reducing roughness and eliminating interface mixing in multilayer X-ray mirrors [6], [7].

The deposition system is mounted on a ultra-high load hexapod with high resolution 6-axis positioning at the High Energy Materials Science P07 beamline at PETRA III [5]. This allows fine alignment of the sample with respect to the synchrotron X-ray beam

enabling time-resolved X-ray diffraction data to be aquired during film growth. In situ wide angle X-ray scattering (WAXS) was performed in transmission mode geometry using a 200 μm high × 700 μm wide X-ray beam at 78 keV, and the diffracted X-rays were collected on a two-dimensional Perkin-Elmer detector at a distance of X m from the sample. Each image was acquired for 160 s, corresponding to ~20 turns of full 360° sample revolution, and the images include diffraction information from a 3D volume of reciprocal space.
X-ray reflectivity measurements were performed on Panalytical Empyrean diffractometer using a Cu X-ray tube, a parallel beam mirror with a 1/32° divergence slit on the primary side, and a parallel plate collimator and a collimator slit (0.27°) on secondary side, together with a PIXcel detector in 0D mode. Reflectivity of single Ni/Ti multilayers doped with B_4C were measured in the range 0°-10° 2θ with a step size of 0.01°/step and a collection time of 1.75 s, giving a total measurement time of ~30 minutes.
Reflectivity simulations were performed using the Panalytical X'pert reflectivity software. The optical constants for (pure) Ni and Ti were used for the multilayers grown without added B_4C, while the optical constants of $Ni_{80}(B_4C)_{20}$ and $Ti_{80}(B_4C)_{20}$ were used for those containing B_4C. In all simulations the densitities of the layers were however fitted to the critical angle. In the simulations a Gaussian interface broadening, the same for each interface, was included to account for interface roughness and intermixing.

Elemental composition was determined for the samples grown with a constant substrate bias voltage using time-of-flight energy elastic recoil detection analysis (ToF-E ERDA) at the Tandem Laboratory at Uppsala university. A 34 MeV $^{127}I^{8+}$ primary beam having an incident angle of 67.5° relative to the surface normal was used, and the energy detector was placed at a recoil scattering angle of 45°. A detailed description of the experimental set-up has been given elsewhere [8], [9]. The measured recoil ToF-E ERDA spectra were analyzed using the CONTES code [10], where the measured recoil energy spectrum of each element was converted to relative atomic concentrations.

X-ray photoelectron spectroscopy (XPS) core-level spectra of B 1s, C 1s, Ni... and Ti… were acquired to analyze the chemical bonding structure of boron and carbon atoms within the layers using an Axis Ultra DLD spectrometer operating at a base pressure of 1.5 × 10^{-7} Pa with monochromatic Al Kα radiation (hν = 1486.6 eV). In order to avoid uncertainties related to commonly used binding energy scale referencing against C *1s* line of adventitious carbon [30], spectra were aligned to the Fermi level cut-off. The spectra were acquired from the 0.3 × 0.7 mm^2 area centered at 3 × 3 mm^2 portion of the sample previously sputter-etched with 0.5 keV Ar ions incident at an angle of 70° from the surface normal. Deconvolution and quantification was performed using the Casa XPS software applying the manufacturer's (Kratos Analytical Ltd.) sensitivity factors [31].

An analytical Tecnai G2 UT FEG microscope operating at 200 kV for a point-to-point resolution of 0.19 nm was used for transmission electron microscopy (TEM) studies. Microstructure and layer definition of Ni/Ti and Ni/Ti doped with B_4C multilayers were studied using both bright field and dark field imaging as well as high resolution cross-sectional TEM. Dark field imaging was used as an approach to effectively highlight crystalline regions in the sample, while high-resolution TEM was used to investigate the layered structure in the multilayers containing the thinnest periods. The cross-sectional samples were prepared using mechanical grinding and polishing followed by low-energy ion-beam milling using a Gatan precision ion polishing system.

Calculations of predicted neutron reflectivity performance has been carried out using the IMD software [11].
SRIM calculations [ref] of Ar ion bombardment of Ni and Ti bilayers, based on the chosen ion assistance growth parameters, support the observed interface phenomena.

3. Results and Discussion

Wide angle X-ray scattering measurements performed after growth on the stacked multilayers are presented in Figure 1. The detector size and distance from the sample allows diffraction from atomic plane distances >X nm to be recorded using 78 keV photons. This corresponds to observing diffraction from the Ni (111) and (002), and Ti (110) and (002) atomic planes, if present. Most of the recorded diffraction spots, however, originate from the crystalline Si substrate and the Al_2O_3 sapphire viewing window, marked in Figure 1 by circles and triangles, respectively.

In Figure 1 a) the 2D X-ray diffraction pattern of a stacked Ni/Ti multilayer grown without B_4C-doping and using a uniform ion assistance by applying a -30 V bias voltage is shown. Apart from substrate and window reflections, strong Ni 111 and faint Ti 002 reflections are visible, showing that the layers under these conditions grow crystalline. Other film reflections are too weak to be observed. Furthermore, since these are diffraction spots, rather than rings, the crystallites are oriented with respect to the substrate. With the Ni 111 in the growth direction and Ti 002 at 45° from the growth direction, the Ni layers are 111 textured while the Ti layers have a 110 texture, as commonly observed for an fcc and a bcc metal, respectively, due to a minimization of the surface energies during growth. This is also consistent with other findings for Ni/Ti multilayers presented in the literature [refs].

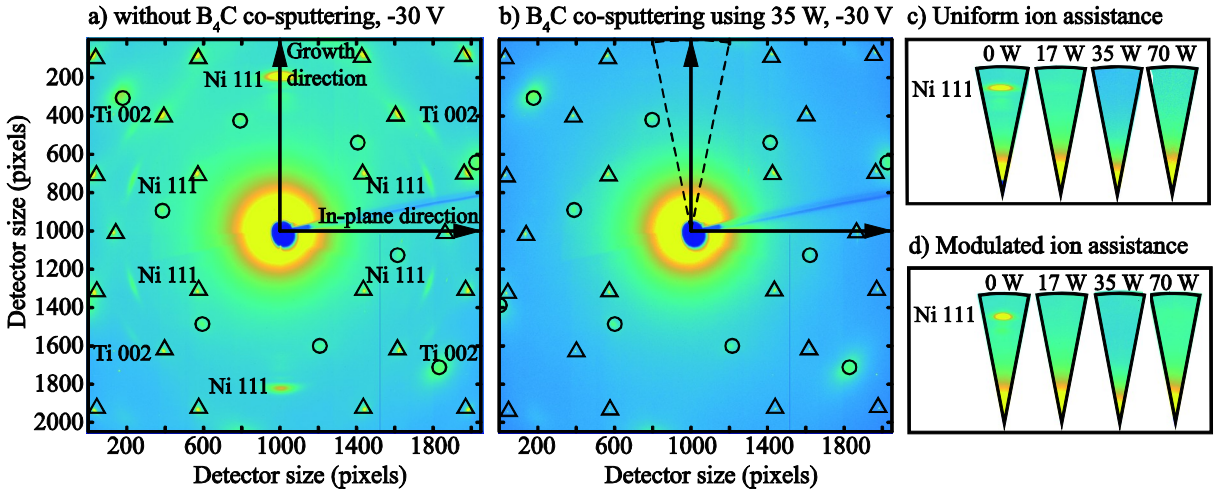

Figure 1. Wide angle X-ray scattering a) without B_4C co-sputtering, b) B_4C co-sputtering using a magnetron power of 35 W, and c) influence of different B_4C powers on the Ni 111-formation in the growth direction.

For growth under the same conditions, except for the addition of B_4C to the multilayer by co-sputtering (using a 35 W magnetron power), diffraction neither from Ni or Ti is observed, as can be seen in the image in Figure 1 b), and the multilayer is considered to be X-ray amorphous. In fact, any addition of B_4C, from the lowest to the highest applied magnetron power, causes the multilayers to be X-ray amorphous, irrespective of the used ion assistance design, as seen from the absence of the Ni 111 reflection in the region around the growth direction in Figures 1 c) and d). Without the addition of B_4C the Ni 111 reflection is present although more well-defined when using a modulated ion assistance, indicating a stronger 111 texture in this case.

Although not clearly visible in the images in Figure 1 c) and d), multilayer reflections are present inside the Ni 111 diffraction spots along the growth direction, showing the presence of a multilayered structure perpendicular to the substrate normal, both for a uniform and a

modulated ion assistance. The reflections are however too few and diffuse to be used to accurately determine the multilayer periods in these stacked multilayers.

In Figure 2 the cross-section of the stacked multilayers, corresponding to those discussed above in Figure 1 a) and b), are shown in bright-field, dark-field and high-resolution TEM micrographs. The nominal multilayer periods are indicated in the bright-field micrograph.

When studying the micrographs for the multilayer grown without B_4C and using a uniform ion assistance in Figure 2, it is seen in a) that the layers are more rough for larger multilayer periods, that the roughness increases with thickness within each multilayer stack, and, for the two thicker periods, that the Ti-on-Ni interface is more rough than the corresponding Ni-on-Ti interface. The asymmetric interface widths for Ni/Ti multilayers have previously been reported in the literature [refs].

From the dark field micrograph in b), the thicker layers are clearly crystalline as seen from the bright regions in the two upper multilayers. The high-resolution micrograph in c) of the thinnest multilayer periods close to the substrate shows that there are crystallites formed also in these thin layers. In addition, the high-resolution micrograph shows that there is no layered structure present.

Explain these observations here:

Larger periods allow facetted Ni and Ti crystallites to grow larger, increasing the interface width. Intermetallics formed at the interfaces. The accumulating roughness can be explained by… crystallite formation, kinetic roughening due to an insufficient adatom surface mobility… while the asymmetric interfaces are due to a forward knock-on effect…. and a difference in displacement energies(?) for Ni and Ti. Diffusion of Ti in Ni..? Probably not diffusion, since the adatoms do not have sufficient kinetic energy. These observations have been made also by other researchers [refs].

The observations of crystalline layers, absence of periodicity in thin period multilayers, formation of interface intermetallics, and an accumulating interface roughness with total multilayer thickness, summarize very well the main features limiting the neutron reflectivity performance of Ni/Ti multilayers.

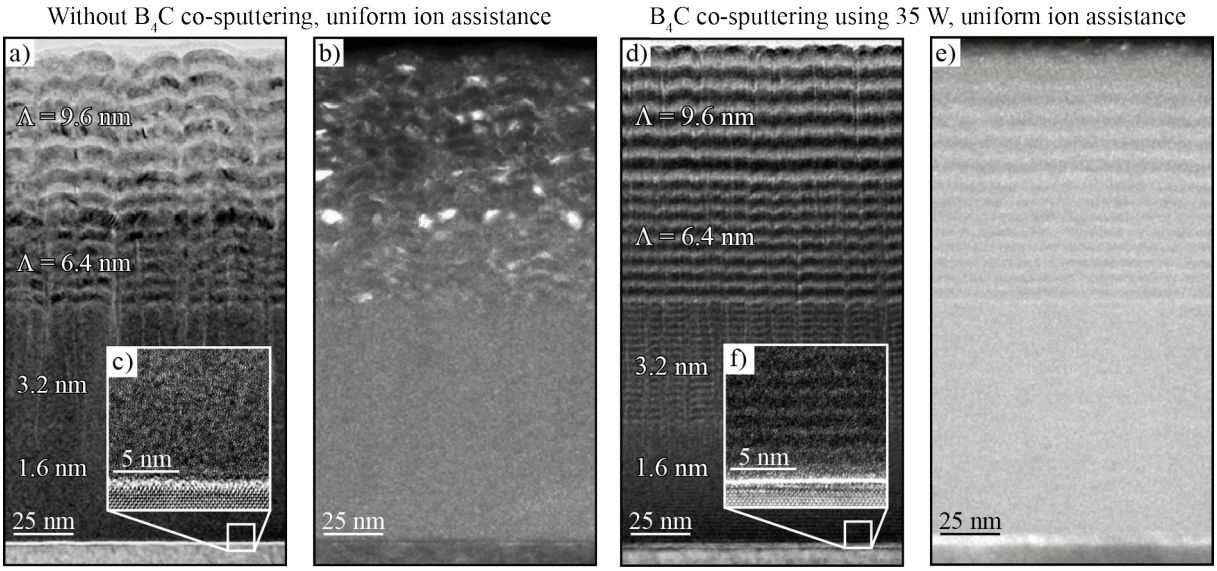

Figure 2. Evolution of crystallinity in stacked Ni/Ti multilayers grown with and without B_4C co-sputtering and a constant ion assistance. a) Bright field micrograph, b) dark field micrograph, c) high-resolution micrograph of a Ni/Ti multilayer grown without B_4C. d) Bright field micrograph, e) dark

field micrograph, and f) high-resolution micrograph of a Ni/Ti multilayer grown using 35 W B_4C co-sputtering.

When introducing B_4C into the Ni/Ti multilayer, Figure 2 d), e), and f), the structure changes significantly. Most obvious is the reduction of the accumulated roughness in d) and the complete absence of any crystallites in f). The high-resolution micrograph of the thinnest layers confirms the formation of an amorphous layer structure throughout the multilayer stack but also that there is a chemical modulation visible for periods as short as 1.6 nm.

Explain these observations here
The amorphization by introducing B and C in to the structure is… due to…

Petrov et al. Microstructural evolution during film growth, J. Vac. Sci. Technol. 2003:
Low-energy ion irradiation during growth is used extensively to overcome the characteristically rough and under-dense microstructures of refractory materials deposited at low Ts (typically Ts/Tm<0.25) [refs]. Under the correct set of deposition conditions, ion bombardment has been shown to increase nucleation rates and film density, to decrease average grain size, to inhibit the formation of columnar structures associated with high surface roughness, and to controllably affect the defect density and orientation of coatings.

[12]

In Figure 3 bright field TEM micrographs of single multilayer structures with a 10 nm periodicity and 5 repetitions are shown in two different length scales to provide both a close-up view and a larger overview of the structures. The crystalline layers with facetted crystallites, and intermetallics at the interfaces are again observed in Figure 3 a) when no B_4C is added and a uniform ion assistance is used. Using B_4C co-sputtering and a constant ion assistance in b), the layers are amorphous but there is an accumulating roughness present indicating that the applied substrate bias voltage results in insufficient adatom mobility leading to a kinetically limited growth. With B_4C co-sputtering and using a modulated substrate bias voltage, with a higher voltage in the end of each layer, shown in c), the layers are amorphous and smooth, and there is no significant accumulated roughness. The improved interface definition using a combination of B_4C co-sputtering and a modulated ion assistance is clearly shown in the overview micrographs in the top of Figure 3.

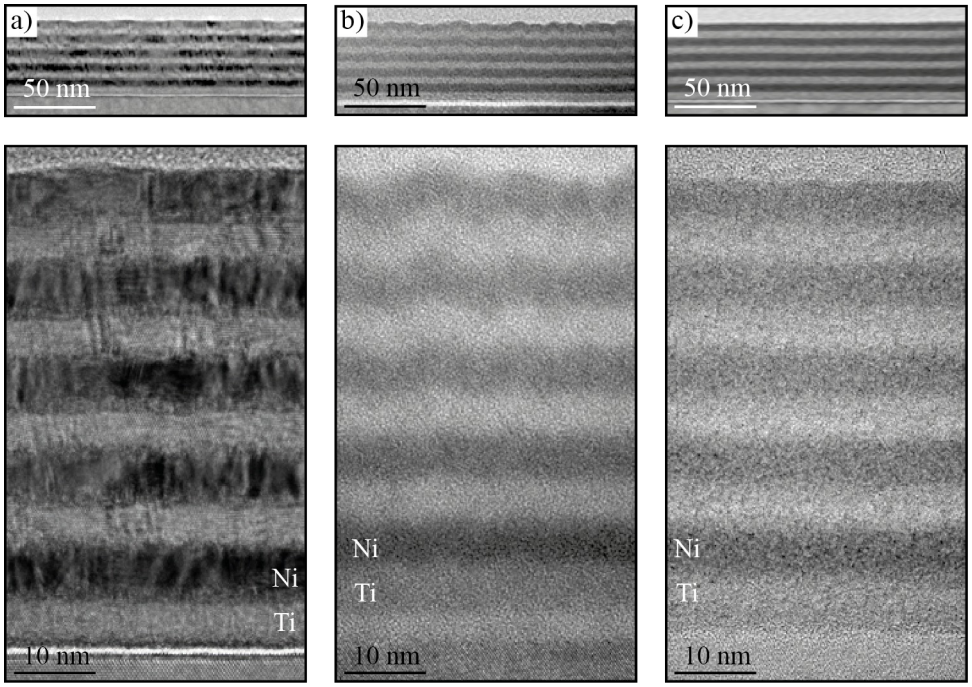

Figure 3. Bright field TEM micrographs of single Ni/Ti multilayers showing the effect of ion assistance. In a) no B_4C is added and a constant ion assistance is applied during growth, while in b) 35 W B_4C co-sputtering is used with a constant ion assistance, and in c) 35 W B_4C co-sputtering and a modulated substrate bias voltage is applied. Overview micrographs are shown on top.

From the wide angle X-ray scattering measurements it was found that the multilayers were X-ray amorphous for all investigated B_4C concentrations. To investigate the influence of the amount of B_4C on the interface quality hard X-ray reflectivity measurements and fitting were employed. In Figure 5 X-ray reflectivity measurements are shown for periodic multilayers, similar to those presented in Figure 3, grown with different ion assistance and increasing B_4C magnetron powers. Since the position of the Bragg peaks are related to the period of the multilayer, the peak shifts towards smaller grazing incidence angles with increasing B_4C magnetron powers shows that an increasing amount of B_4C is being incorporated. For both a constant and a modulated ion assistance the periods increase linearly from about 9.7 nm to about 11.5 nm, i.e. by almost 19 %, when increasing the B_4C magnetron power up to 70 W.

Since the reflectivity profiles represent the Fourier transform of the electron density variation along the growth direction, more and sharper Bragg peaks qualitatively correspond to more well-defined interfaces that are more abrupt and flat, and the regular appearance of Kiessig fringes is an evidence of a high layer thickness uniformity.

When using B_4C co-sputtering and a constant ion assistance it can be seen from the reflectivity measurements in Figure 5 a) that there are fewer Bragg peaks with lower intensities and more irregular Kiessig fringes when the amount of B_4C in the multilayer is increased. Thus, even though the multilayers turn amorphous, the B_4C doping deteriorate the multilayer structure. This is due to an effective reduction of the adatom mobility by formation of more metal boride and carbide bonds when increasing the amount of B and C atoms in the multilayer, in combination with an insufficient ion assistance due to a too low ion energy. The low adatom mobility cause interface roughness which can not be counteracted by the applied substrate bias voltage.

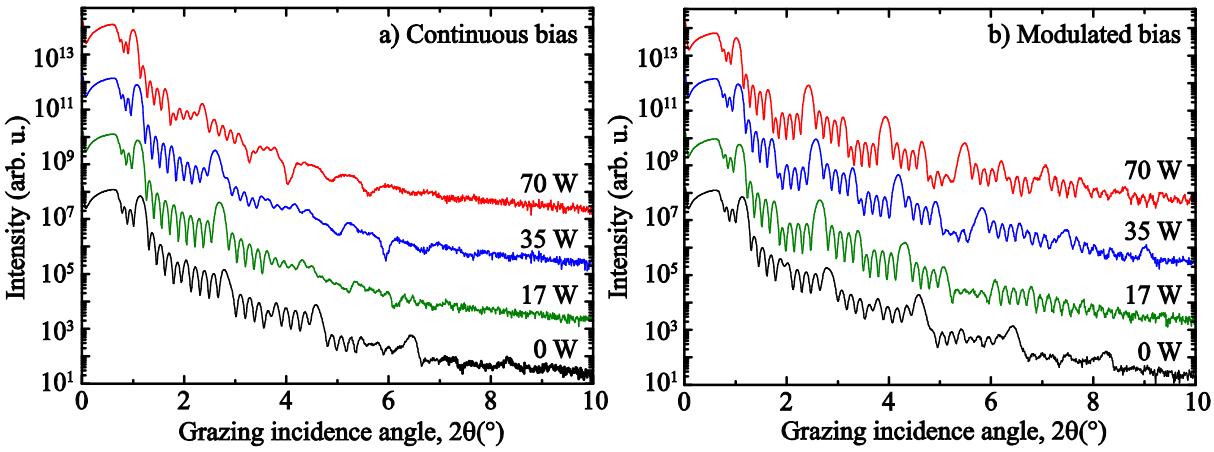

Figure 4. X-ray reflectivity measurements of multilayers grown using a) a constant ion assistance, and b) a modulated ion assistance. Vertically shifted for clarity.

When applying a modulated ion assistance with a higher ion energy in the end of each layer the resulting interface morphology evolution with increasing amount of B_4C incorporation is completely different. Without addition of B_4C (0 W magnetron power) the reflectivity profiles are almost identical. However, with increasing B_4C the trend is now instead towards more Bragg peaks with higher intensities and more clear Kiessig fringes, indicating improved interface qualities with more B_4C.

The low ion energy assistance in the beginning of each layer allows for the formation of an abrupt, although rough and porous, initial part of each layer, while the higher ion energy in the end of each layer provides forward knock-on densification and an increasing adatom surface mobility for a smooth top surface for the deposition of the next layer [ref Ni/V].

Thus, as seen from these results, when B_4C co-sputtering is used for layer amorphization, a modulated ion assistance is not only beneficial for the interface structure, but is in fact necessary for the formation of … high quality multilayers.

Use SRIM (or the analytical calculations) to verify the chosen bias voltages – see what happens with these voltages/energies.

To confirm the qualitative observations made above fittings were made to the measured reflectivity profiles to quantitatively obtain the individual interface widths of Ni and Ti for the different growth conditions. Although an accumulating roughness is evident from the transmission electron microscopy studies, the same interface width have been applied throughout the multilayer stack in the simulations, effectively resulting in an overestimated average interface width. The results are illustrated with the interface width as a function of the B_4C magnetron power in Figure 5 a) for constant ion assistance and in b) for a modulated ion assistance, respectively.

The interface width is always smaller when using a modulated ion assistance, also without B_4C incorporated in the multilayer.

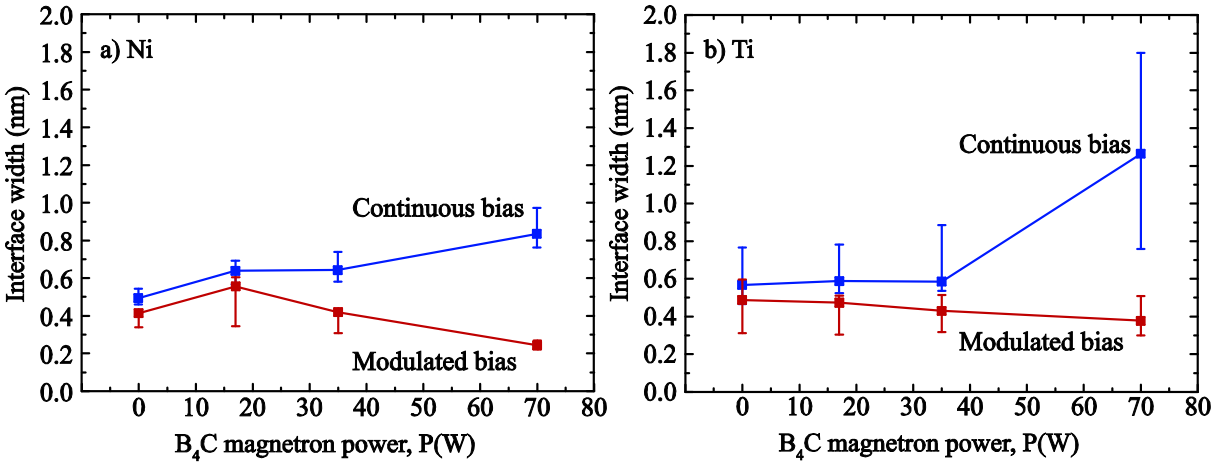

Figure 5. Interface width evolution with increasing B_4C magnetron power.

B4C + modulated assistance →significantly reduced interface widths.

XPS

Due to the mixing caused by the Ar(?) sputtering ions used for depth profiling it is not possible to extract any interface width.

In the depth profile of the multilayer grown with a 70 W magnetron power B4C co-sputtering, it was found that the average B/C ratio is 4.3 for the top multilayer period.
The different depth scales are due to different sputtering yields for the etching. Without B4C the sputtering rate is 6.5 Å/min, while with B4C the sputtering rate is reduced to 4.9 Å/min. This indicates that the sputtering yield has decreased with B and C in the layers, indicating the formation of metal boride and carbide bonds, that have higher surface binding energies than for the pure elements.

Chemical shift for the Ni 2p photoelectron peak towards higher binding energies inside the Ti layer shows Ni implanted into Ti (during depth profiling, or during deposition?) Similarly for the Ti 2p peak.
Ti-B bonds inside the Ti layer. C-B bonds indside the Ni layers. Compare enthalpies of formation..

C-Ti inside Ti layer.

Brasklapp: Some residual C implanted into Ni and Ti due to Ar+ etch
Some TiC and NiC formed due to Ar+ etch.

Figure 6. X-ray photoelectron spectroscopy results -depth profiling + chemical shifts representing the metal boride and carbide bonding…

These numbers can be used to predict the performance of the neutron reflectivity performance.

Predicted performance of Ni/Ti-based supermirrors

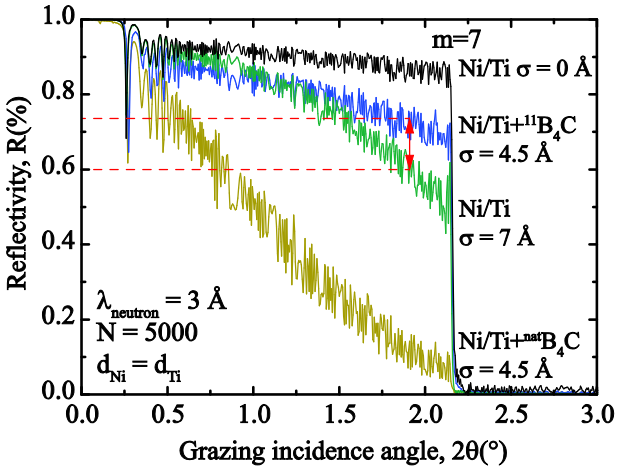

Figure 7. Supermirror performance

Significantly increased waveguide transmission expected with Ni/Ti+11B4C. Good prospects for long, high reflectivity, high-m, supermirrors for waveguides.
Ta med fler än Ni/Ti, NiTiB4C, …?

4. Discussion

4.1 Film growth and microstructure

4.2 Evolution of crystallinity in Ni/Ti multilayers

4.3 Neutron optical properties

Here in this work we have only used a low number of layers in order to investigate the concept of B4C-doping and ion-assisted growth to improve the interfaces. […] We should mention stress-reduction with amorphous Ni/Ti multilayers. This enables more layers to be deposited, and thus facilitates supermirrors with higher m-values.

B_4C + modulated assistance → significantly reduced interface widths.

Hard X-ray reflectivity simulations indicate interface widths of about 4.5 Å

When looking closer at the interfaces in Figure 6 c) they are very smooth, but they seem to be quite intermixed.

Reducing the intermixing could thus lead to a further improvement in interface quality.

Could it be that the 100 eV ion bombardment in the end of each layer is too large, causing a forward knock-on effect leading to interface mixing?

5. Conclusions

Here the concept for layer morphology control using B4Cin Ni/Ti multilayer mirrors have been

Ni/Ti with B4C → X-ray amorphous
Pure Ni/Ti multilayers are crystalline and have a 111 texture. Using a modulated bias voltage the texture is stronger.

Acknowledgements
Mit VR?

Captions

Figure 1. XRD diffractograms for cubic CrN deposited at 600, 650 and 700 $^{\circ}C$. a) The gas flow is set to 21 *sccm* nitrogen and 33 *sccm* argon (40% nitrogen) resulting in single phase CrN. The inset is a pole figure for cubic CrN deposited on sapphire at 700 $^{\circ}C$. b) The gas flow is set to 11 sccm nitrogen and 33 sccm argon (20% nitrogen) resulting in the formation of hexagonal Cr_2N.

Figure 2.

Figure 3.

Figures

References

[1] D. Liu, B. Khaykovich, M.V. Gubarev, J. Lee Robertson, L. Crow, B.D. Ramsey, D.E. Moncton, Demonstration of a novel focusing small-angle neutron scattering instrument equipped with axisymmetric mirrors, Nat Commun, 4 (2013) 2556.
[2] T. Veres, S. Sajti, L. Cser, S. Bálint, L. Bottyán, Roughness replication in neutron supermirrors, Journal of Applied Crystallography, 50 (2017) 184-191.
[3] S.a. Bajt, Improved reflectance and stability of Mo-Si multilayers, Optical Engineering, 41 (2002).
[4] N. Ghafoor, F. Eriksson, A. Aquila, E. Gullikson, F. Schafers, G. Greczynski, J. Birch, Impact of B4C co-sputtering on structure and optical performance of Cr/Sc multilayer X-ray mirrors, Opt Express, 25 (2017) 18274-18287.
[5] J.L. Schroeder, W. Thomson, B. Howard, N. Schell, L.A. Naslund, L. Rogstrom, M.P. Johansson-Joesaar, N. Ghafoor, M. Oden, E. Nothnagel, A. Shepard, J. Greer, J. Birch, Industry-relevant magnetron sputtering and cathodic arc ultra-high vacuum deposition system for in situ x-ray diffraction studies of thin film growth using high energy synchrotron radiation, Rev Sci Instrum, 86 (2015) 095113.
[6] F. Eriksson, N. Ghafoor, F. Schafers, E.M. Gullikson, J. Birch, Interface engineering of short-period Ni/V multilayer X-ray mirrors, Thin Solid Films, 500 (2006) 84-95.
[7] F. Eriksson, F. Schafers, E.M. Gullikson, S. Aouadi, N. Ghafoor, S. Rohde, L. Hultman, J. Birch, Atomic Scale Interface Engineering by Modulated Ion Assisted Deposition Applied to Soft X-ray Multilayer Optics, Applied Optics, DOI (2008).
[8] H.J. Whitlow, G. Possnert, C.S. Petersson, Quantitative mass and energy dispersive elastic recoil spectrometry: Resolution and efficiency considerations, Elsevier, Nuclear Instruments and Methods in Physics Research Section B: Beam Interactions with Materials and Atoms, 27 (1987) 448-457.
[9] J. Jensen, D. Martin, A. Surpi, T. Kubart, ERD analysis and modification of TiO2 thin films with heavy ions, Nuclear Instruments and Methods in Physics Research Section B: Beam Interactions with Materials and Atoms, 268 (2010) 1893-1898.
[10] M.S. Janson, CONTES, Conversion of Time-Energy Spectra, a program for ERDA data analysis, Internal Report, Uppsala University, DOI (2004).
[11] D.L. Windt, IMD—Software for modeling the optical properties of multilayer films, Computers in Physics, 12 (1998).
[12] W. Li, J. Zhu, H. Li, Z. Zhang, X. Ma, X. Yang, H. Wang, Z. Wang, Ni layer thickness dependence of the interface structures for Ti/Ni/Ti trilayer studied by X-ray standing waves, ACS Appl Mater Interfaces, 5 (2013) 404-409.